ACS APPLIED MATERIALS & INTERFACES

Research Article

www.acsami.org

Epitaxial Growth of an Organic p–n Heterojunction: C_{60} on Single-Crystal Pentacene

Yasuo Nakayama,[*,†] Yuta Mizuno,[‡] Takuya Hosokai,[§] Tomoyuki Koganezawa,[∥] Ryohei Tsuruta,[†] Alexander Hinderhofer,[⊥] Alexander Gerlach,[⊥] Katharina Broch,[#] Valentina Belova,[⊥] Heiko Frank,[⊥] Masayuki Yamamoto,[‡] Jens Niederhausen,[○,▽] Hendrik Glowatzki,[▽] Jürgen P. Rabe,[○] Norbert Koch,[○,▽] Hisao Ishii,[‡,□] Frank Schreiber,[⊥] and Nobuo Ueno[‡]

[†]Department of Pure and Applied Chemistry, Faculty of Science and Technology, Tokyo University of Science, 2641 Yamazaki, Noda, Chiba 278-8510, Japan

[‡]Graduate School of Advanced Integration Science, Chiba University, 1-33 Yayoi-cho, Inage-ku, Chiba 263-8522, Japan

[§]National Metrology Institute of Japan, National Institute of Advanced Industrial Science and Technology, Tsukuba Central 2, 1-1-1 Umezono, Tsukuba, Ibaraki 305-8568, Japan

[∥]Industrial Application Division, Japan Synchrotron Radiation Research Institute (JASRI), 1-1-1 Kouto, Sayo, Hyogo 679-5198, Japan

[⊥]Institut für Angewandte Physik, Eberhard Karls Universität Tübingen, Auf der Morgenstelle 10, 72076 Tübingen, Germany

[#]Cavendish Laboratory, University of Cambridge, Cambridge CB3 0HE, U.K.

[○]Institut für Physik & IRIS Adlershof, Humboldt-Universität zu Berlin, Newtonstr. 15, DE-12489 Berlin, Germany

[▽]Helmholtz Zentrum Berlin für Materialien und Energie GmbH, Albert-Einstein-Strasse 15, DE-12489 Berlin, Germany

[□]Center for Frontier Science, Chiba University, 1-33 Yayoi-cho, Inage-ku, Chiba 263-8522, Japan

Supporting Information

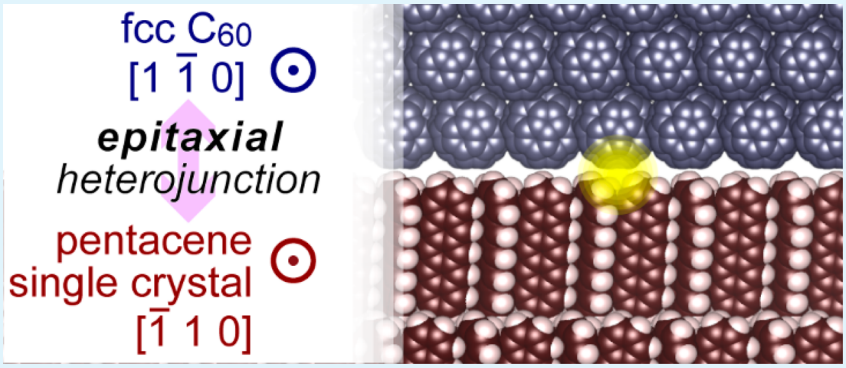

ABSTRACT: Designing molecular p–n heterojunction structures, i.e., electron donor–acceptor contacts, is one of the central challenges for further development of organic electronic devices. In the present study, a well-defined p–n heterojunction of two representative molecular semiconductors, pentacene and C_{60}, formed on the single-crystal surface of pentacene is precisely investigated in terms of its growth behavior and crystallographic structure. C_{60} assembles into a (111)-oriented face-centered-cubic crystal structure with a specific epitaxial orientation on the (001) surface of the pentacene single crystal. The present experimental findings provide molecular scale insights into the formation mechanisms of the organic p–n heterojunction through an accurate structural analysis of the single-crystalline molecular contact.

KEYWORDS: *grazing-incidence X-ray diffraction, X-ray reflectivity, synchrotron radiation, organic semiconductor, fullerene, organic electronics, solar cell, van der Waals epitaxy*

1. INTRODUCTION

The controlled formation of p–n junctions is one of the most crucial subjects in semiconductor technology. In the emerging field of organic optoelectronics, the term "p–n junction" almost always refers to a donor–acceptor molecular contact between two kinds of π-conjugated (organic) semiconductors. The development of efficient organic electronic devices is supported by improved designs of organic p–n heterojunctions, particularly in the case of organic photovoltaic (OPV) devices. Beginning from a simple donor–acceptor bilayer structure,[1]

Received: March 4, 2016
Accepted: May 12, 2016
Published: May 12, 2016

DOI: 10.1021/acsami.6b02744
ACS Appl. Mater. Interfaces 2016, 8, 13499–13505

introduction of the bulk-heterojunction concept led to a revolutionary improvement in the performance of OPVs.[2−4] The technology for shaping the architecture within bulk heterojunctions has evolved from the submicrometer scale[5] toward individual molecular contacts.[6] One fundamental requirement to realize molecular-scale engineering of organic p−n heterojunctions is a detailed insight into the behavior of organic molecules in contact with other materials.[7] Static and dynamic properties of the molecular layers can be inferred from the interface structures and their evolution on uniform and well-defined surfaces of molecular crystals.[8−21] However, in the case of heterojunctions made of molecular semiconductors, high-precision studies, namely using organic single crystals as substrates, have been quite limited so far.[9,13,17,19]

In the present work, a well-defined organic p−n heterojunction was prepared by depositing C_{60} overlayers onto the surface of single crystal substrates of pentacene ($C_{22}H_{14}$), and its growth behavior and crystallographic structures were precisely analyzed using scanning probe microscopy and surface X-ray diffraction techniques. Pentacene and C_{60} are widely employed p-type and n-type molecular semiconductors, respectively. The heterojunction of these two materials is known to constitute the exciton dissociation interface in an OPV device of a basic structure,[22] and many experimental and theoretical studies have been targeted toward characterizing their physical properties and functionalities.[23−31] On the other hand, it needs to be pointed out that these materials are respectively quite attractive also because of their distinct characteristics that make them stand out among common organic semiconductors; for instance, C_{60} is an exceptional molecule by its high symmetry in terms of the bulk crystal phase as well as the molecular shape, and pentacene is known to exhibit singlet exciton fission very efficiently making this molecule quite promising for high performance OPV devices via overcoming of the exciton diffusion bottleneck.[32,33] Recently, the electronic structures of the C_{60}-pentacene heterojunction assembled onto the single crystal surface of pentacene were reported.[34] In that work, the formation of a well-ordered crystalline C_{60} overlayer was only inferred from the observed interface morphology. Accurate structural analysis using established surface science methodologies was now conducted to disclose the crystallographic structures of this p−n heterojunction formed by epitaxial assembling C_{60} on the pentacene single-crystal surface.

2. EXPERIMENTAL SECTION

Pentacene single crystals (Pn-SCs) were grown by horizontal physical vapor transport in a purified nitrogen stream. Typically, several-micrometer-square and few-micrometer-thick plate-shaped Pn-SCs were selected and, in ambient conditions, attached onto Si wafers coated with the native oxide to prepare the samples. The crystalline phase of the present Pn-SC samples is the one of 1.41 nm layer periodicity among the four known crystalline polymorphs of pentacene,[35,36] and their surfaces are known to be either the (001) or the (00$\bar{1}$) planes.[35,37] No surface treatment was carried out for these samples and therefore, the Pn-SC samples used in the present case likely contained surface oxidized species in the order of a few percent.[38] C_{60} source material (99.98%) was purchased from ATR Company and was used as received. C_{60} was evaporated from carefully degassed quartz or carbon crucibles to form the heterojunction on the Pn-SC surface at room temperature. The evaporation rate was monitored with a quartz microbalance and controlled to be of the order of 0.1 nm/min calibrated by either a step profiler or in-house X-ray reflectivity measurements.

The surface morphology of the heterojunction was observed by noncontact mode atomic force microscopy (nc-AFM) [VT-SPM, Omicron Nanotechnology] in ultrahigh vacuum (UHV) condition. The details of the experimental setup can be found elsewhere.[17] X-ray reflectivity (XRR) measurements were conducted at the MS Surface Diffraction beamline[39] of Swiss Light Source with an X-ray energy of 14.0 keV. For the XRR experiments, C_{60} deposition was done "on-site" and in a stepwise manner using a home-built portable UHV chamber with a Be window[40,41] that permitted tracking the in situ evolution of the heterojunction structures. Two-dimensional grazing-incidence X-ray diffraction (2D-GIXD) experiments were carried out at BL19B2 and BL46XU of SPring-8 by using PILATUS300 K or PILATUS100 K as two-dimensional X-ray detectors. The X-ray energy and glancing angle were fixed at 12.4 keV and 0.12°, respectively, and the in-plane azimuthal angle of the sample to the surface normal (the c^* axis of the Pn-SC) was rotated. The experimental setup for the 2D-GIXD measurements is illustrated in Figure S1. Note that the 2D-GIXD experiments were conducted in air on samples prefabricated in a separate UHV system. All the experiments throughout C_{60} deposition to nc-AFM, XRR, or 2D-GIXD measurements were conducted at room temperature.

3. RESULTS AND DISCUSSION

Figure 1a shows the typical surface morphology of the Pn-SC observed by nc-AFM in UHV. Flat and uniform terraces of

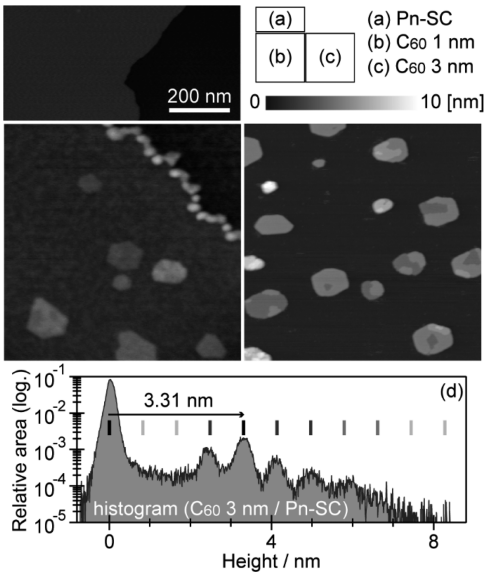

Figure 1. In situ AFM topographies of the Pn-SC (a) before and after coverage of (b) 1 nm and (c) 3 nm thick C_{60} overlayers. The lateral and vertical dimensions are the same for these three images. (d) The height distribution plotted in the logarithmic vertical scale extracted from a wider-field AFM image (including the area of Figure 1c) of the Pn-SC covered by 3 nm thick C_{60}. The height scale is calibrated by using the single molecular step (1.41 nm) of the Pn-SC surface. The vertical bars represent the expected scale for C_{60} molecular layers (see corresponding description in the text).

micrometer-scale width are seen that are divided by step edges of single-molecular heights. Deposition of a small amount of C_{60} (nominally 1 nm) resulted in a change in the surface morphology as shown in Figure 1b. The step edges were fully decorated by protrusions with heights of typically (6 ± 1) nm as measured from the lower terrace. Aggregation of adsorbed C_{60} molecules on the surface of "thin-film phase" crystalline pentacene has been reported.[29] Molecular dynamics calculations have predicted that C_{60} molecules burrow into the Pn-

DOI: 10.1021/acsami.6b02744
ACS Appl. Mater. Interfaces 2016, 8, 13499−13505

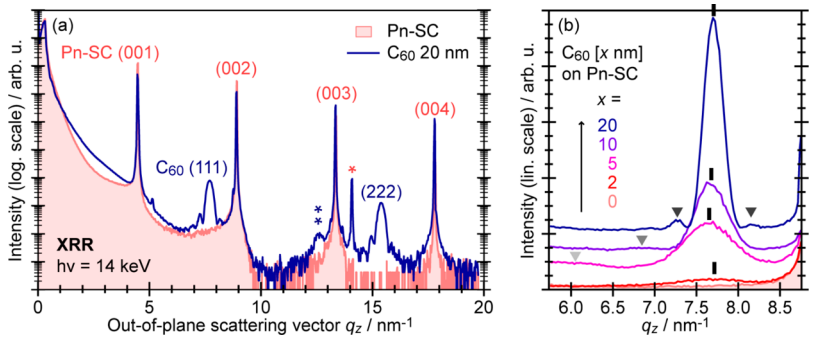

Figure 2. (a) In situ XRR spectra of the Pn-SC before and after deposition of 20 nm-thick C_{60} overlayer plotted in the logarithmic scale (vertical axis). (b) Evolution of the in situ XRR spectra with increasing C_{60} thickness (plotted in the linear scale). The peak positions of the C_{60}(111) Bragg reflection and its Laue fringe structures are marked with vertical bars and downward triangles, respectively.

SC lattice on the surface of the (010) plane.[30,42] Similar to the (010) surface, the "ventral side" of each pentacene molecule faces outside at the step edges. Therefore, the protrusions decorating the step edges should be attributed to Pn-C_{60} mixtures or, presumably, to intermolecular compounds formed from the two materials.[31]

Even though these step-edge species have potential importance because of the strong donor−acceptor interaction, they have to be minor in terms of the molecular population out of the whole surface. Another characteristic feature found on this surface is the presence of "islands" interspersed on the terraces of the Pn-SC. As seen in Figure 1b, the width distribution of these islands range from several tens to hundreds of nm and the height is less than 4 nm from the surface of the terrace. In addition, these islands have relatively flat tops and straight rims suggesting a different internal structure from that of the protrusions at the step edges. Such a regular shape for a C_{60} overlayer was previously observed on pentacene thin films formed on sapphire(0001) surface,[23] but is contrary to the case where formation of C_{60} clusters was reported on pentacene/SiO_2.[27] Increase in the nominal thickness of C_{60} to 3 nm raised the height of the islands on the terraces and the number density of the islands, as shown in Figure 1c, whereas any lateral elongation was small. The top surfaces of most of the islands were extremely smooth and it was possible to identify the "step edges" within individual islands. Figure 1d shows the height distribution of a single Pn-SC terrace derived from a wider area AFM image of the Pn-SC covered with the 3 nm-thick C_{60} overlayer. Modulations with a periodicity of (0.84 ± 0.04) nm are clearly observed. This periodicity corresponds fairly well to the molecular diameter of C_{60} and is actually identical to the lattice spacing of the (111) plane of the face-centered cubic (fcc) C_{60} crystal (0.823 nm[43]). These observations imply that these islands consist of well-crystallized C_{60}. As indicated in Figure 1d, the most probable height of the islands, (3.31 ± 0.10) nm from the terrace surface of the Pn-SC, corresponds to four molecular layers of the (111)-oriented fcc C_{60} crystal. In the present results, islands of three up to eight molecular layers high were found, whereas, interestingly, those of one or two layers are rarely formed. This might be due to the fact that at least three layers are essential to construct the fcc structure (see Figure S2).

Further increasing the C_{60} thickness to 6 nm leads to the complete coverage of the Pn-SC surface by the C_{60} islands (as seen in Figure S3). Previously, based on X-ray photoemission data, we have proposed that C_{60} grows in the Volmer−Weber mode on the Pn-SC surface and the critical thickness at which the Pn-SC surface is totally covered by the C_{60} overlayer is around 5 nm.[34] The present results provide a clear evidence for this proposed growth manner.

The XRR data of a Pn-SC sample before and after coverage of the 20 nm thick C_{60} overlayer showed four very sharp and intense Bragg peaks at the out-of-plane scattering vector (q_z) positions of $(4.45 \times n)$ nm^{-1} (Figure 2a). These peaks are attributed to the $(00n)$ Bragg reflection from the Pn-SC as marked in the figure. The lattice spacing derived from the peak position is 1.410 nm, which is in excellent agreement with the reported crystal structure of pentacene (1.412 nm[44]). On the XRR curve of the C_{60}-covered sample, peaks at $q_z \approx (7.7 \times n)$ nm^{-1} appeared. These q_z values correspond to a lattice spacing of 0.816 nm, which coincides with the aforementioned (111) layer distance of the fcc C_{60} crystal. Therefore, it is concluded that the C_{60} molecules assemble themselves with the (111)-plane parallel to the Pn-SC surface as previously reported also on crystalline thin films of pentacene.[16] The sharp peak at $q_z \approx$ 14.0 nm^{-1} (marked with a single asterisk sign) and the broader one at $q_z \approx$ 12.5 nm^{-1} (double asterisk) can be attributed to misoriented crystallites of pentacene and adsorbed C_{60} onto these crystallites, respectively.

Figure 2b shows the evolution of the C_{60}(111) Bragg reflection as a function of the C_{60} thickness. The peak position was confirmed from a 2 nm-thick C_{60} film and was maintained at q_z = (7.70 ± 0.05) nm^{-1} throughout the thickness range. This indicates that C_{60} crystallizes into a structure that is compatible with its fcc bulk phase in regions of low thicknesses, i.e. even before completely covering the surface. Besides, it is clearly seen that the main Bragg peak is accompanied by the Laue oscillations as indicated by downward triangles in the figure. The coherent thicknesses as estimated from these fringe structures are (3.9 ± 0.6) nm, (7.6 ± 1.3) nm, and (14.1 ± 1.4) nm for 5, 10, and 20 nm thick C_{60} overlayers, respectively. These values agree with the nominal thicknesses of the corresponding C_{60} overlayers fairly well, which also confirms the good crystallinity of C_{60} over the entire thickness range.

The XRR data indicate that the *a* and *b* axes of the Pn-SC and the $[\bar{1}10]$ direction of the (111)-oriented fcc C_{60} overlayer are in the same plane. Therefore, the interrelation between these in-plane axes of the Pn-SC and fcc C_{60} was explored using 2D-GIXD. Even though the results represented above were obtained from "in-situ" experiments, (where the deposition of the C_{60} overlayer and the measurements were both conducted under UHV condition without breaking the vacuum), nc-AFM observations prove that the exposure of these samples to ambient air and light does not impact the morphology of the

DOI: 10.1021/acsami.6b02744
ACS Appl. Mater. Interfaces 2016, 8, 13499−13505

C_{60}-induced structures (see Figure S3). In addition, it will be shown below that the crystallinity of the C_{60} overlayer is not changed by exposure to ambient conditions.

Figure 3a shows 2D-GIXD data for a Pn-SC with a 20 nm C_{60} overlayer; the data have been integrated over the sample

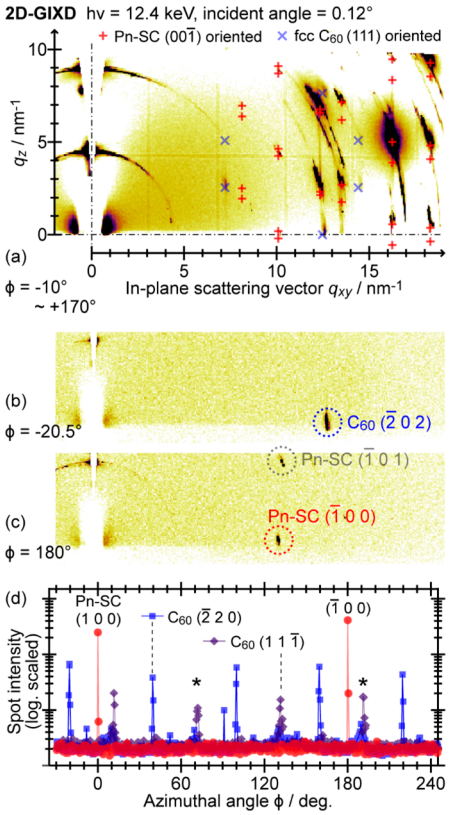

Figure 3. (a) Ex situ 2D-GIXD image of Pn-SC covered with 20 nm thick C_{60} integrated for sample azimuthal angles from 0° to 180° (360 images taken with a step size of 0.5°). Expected positions for the diffraction spots of the (00$\bar{1}$) oriented Pn-SC and (111) oriented fcc C_{60} single crystal are marked with + and × signs, respectively. (b, c) Single shot 2D-GIXD images taken at specific azimuthal angles. (d) Intensity distribution of three representative diffraction spots depending on the sample azimuthal angle.

azimuthal angle ϕ in the range of 180°. Although these images were obtained under ambient conditions (ex situ), the diffraction spots from both the crystalline C_{60} overlayer and the Pn-SC are clearly defined. The q positions of the observed spots are reproduced assuming the fcc unit-cell structure of C_{60}[43] and Pn bulk single crystal.[44] As shown in single shot 2D-GIXD images (Figure 3b, c), each diffraction spot appeared only at specific ϕ and is absent for other azimuthal angles. For instance, a diffraction spot assigned to the C_{60} overlayer emerged at $\phi = -20.5°$ (Figure 3b) is completely absent for other angles (e.g., $\phi = 180°$; Figure 3c). This observation strongly suggests that the C_{60} overlayer is not polycrystalline but that its lattice is preferentially oriented in specific directions.

The intensities at the three q positions, (q_{xy}, q_z) = (10.1 nm^{-1}, 0 nm^{-1}), (12.5 nm^{-1}, 0 nm^{-1}), and (7.2 nm^{-1}, 2.5 nm^{-1}), are plotted as a function of ϕ in Figure 3(d). The first q position corresponds to either the (100) or ($\bar{1}$00) reflection of the Pn-SC and appeared at an interval of 180° as expected. After analyzing the spot profile (see Figure S4), the diffraction spots at ϕ = 0 and 180° are individually assigned to (100) and ($\bar{1}$00), respectively. The second position comes from the ($\bar{2}$20) reflection of the (111)-oriented C_{60} crystal and its crystallographically equivalent planes with a periodicity of 60° in ϕ. This correlates with the hexagonal lattice of the (111) surface of the fcc structure of C_{60}, and indicates that the closed-packed C_{60} overlayer grows with a specific epitaxial relationship to the Pn-SC substrate. The third q position, (11$\bar{1}$) and its equivalent reflections, has the same periodicity in ϕ. The expected periodicity from the point of view of crystallography is 120° rather than 60°, and the diffraction spots with asterisks in Figure 3(d) cannot be indexed under the assumption of a single crystalline orientation. This suggests the probable coexistence of crystalline twin variants rotated 180° with respect to each other, namely "ABC" and "ACB" stacked hexagonal molecular layers of C_{60} in the overlayer (schematically drawn in Figure S2). It should be emphasized that the C_{60} molecular arrangement at the first interfacial layer is assumed to be identical for the "ABC" and "ACB" variants.

As indicated in the 2D-GIXD results, the sample azimuthal angle that fulfills the diffraction condition for the [$\bar{1}$10] direction of the (111)-oriented C_{60} crystal is at 39.5° (±0.5°) counterclockwise to that of the Pn-SC (100) scattering. An interlattice relationship between the Pn-SC and the hexagonally packed C_{60} first layer can be derived by a geometric interpretation of the diffraction conditions from the reciprocal to the real space. In the present heterojunction, the nearest-neighbor direction of the hexagonal C_{60} lattice (e.g., [$\bar{1}$10]) is not aligned along the lattice of the Pn-SC in contrast to results in a previous study on a C_{60} overlayer on a tetracene single crystal.[19] Instead, in our case, the nearest-neighbor direction of the hexagonal C_{60} lattice is rotated by 5.3° clockwise with respect to the "primary" axis (which is parallel to the a axis) of the Pn-SC. In strict sense, the direction of the "primary" axis is not sufficient for a unique determination of the crystallographic orientation of the Pn-SC substrate because the (00$\bar{1}$) surface of the triclinic Pn-SC is not equivalent to the (001) surface. These two sides can be distinguished from the diffraction conditions for the secondary axis, namely (01n). As illustrated in Figure S5, the surface of Pn-SC in the present case is determined to be the (00$\bar{1}$) face, and in order to unambiguously represent this point, we take the "primary axis" of the Pn-SC to be in the minus a direction for this crystal. Altogether, an interlattice relation of the topical heteroepitaxial interface is uniquely determined as shown in Figure 4. It is noteworthy that one lattice point (marked with a broken circle) of the surface primitive cell of the closed-packed C_{60} layer is located very close to a diagonal point of the two-dimensional unit cell of the Pn-SC; a lattice mismatch of these two is estimated to be 5.9% under assumption of the lattice constant by respective bulk crystallographic values.[43,44] A coincidence of the reciprocal lattice points of the Pn-SC and C_{60} is also derived from this lattice model, and this conclusion is confirmed by the 2D-GIXD image shown in Figure S6.

Although one pair of lattice points of the Pn-SC and the C_{60} overlayer coincides well, this heterojunction should still be classified as the incommensurate according to the rules of the "grammar of epitaxy".[45] Actually, no commensurate relationships are crystallographically realistic for the present combination because the degree of symmetry of the triclinic Pn-SC substrate is very low in comparison to the highly symmetric C_{60} crystal. Epitaxial growth of such heterojunctions despite considerable lattice mismatch between the adsorbate and substrate can be understood in the framework of what has

DOI: 10.1021/acsami.6b02744
ACS Appl. Mater. Interfaces 2016, 8, 13499−13505

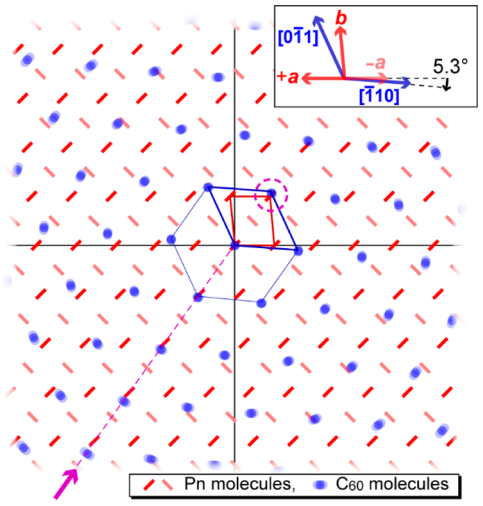

Figure 4. A schematic drawing of the interlattice relationship in the topical molecular semiconductor heterojunction. The surface molecular arrangement of the Pn-SC is shown by bars where two inequivalent molecules in a unit cell are distinguished by the direction of the marks. The circles represent the in-plane arrangement of the C_{60} molecules in the first interface layer, where a "blur" in each mark corresponds to uncertainty in the azimuthal angle. The two-dimensional primitive cells of the Pn-SC and the closed-packed C_{60} layer are indicated by parallelograms, where the hexagonal molecular arrangement of the latter is indicated with thin lines. The origins of the lattices are aligned at the center indicated by the cross-hairs. (Inset): An interrelation between the characteristic axes of the Pn-SC and C_{60} overlayer.

been called van der Waals epitaxy which is applied when there is no strong chemical bond at the heterojunction.[46,47] The lattice of the C_{60} overlayer is oriented in a way so as to reduce the total energy at the heterojunction; this is achieved through the coincidence of the reciprocal points (Figure S6).[48]

It is worth pointing out that the present epitaxial relation shown in Figure 4 is not the only solution for minimizing the lattice mismatch but a comparable or rather smaller mismatch value (3.3%) is expected if one aligns the nearest-neighbor direction of C_{60} to the [110] direction, rather than [1$\bar{1}$0], of the Pn-SC. Despite this circumstance, any diffraction spots assignable to the latter possibility were absent in the present 2D-GIXD results. This fact implies that the minimization of the lattice mismatch may not be the principal criterion to determine the orientations of general van der Waals epitaxy systems. At least for the present heterojunction, another factor lines up the C_{60} molecules on the Pn-SC surface. In this context, it is interesting to note that the anisotropic diffusion of the C_{60} molecule along the [1$\bar{1}$0] direction on the Pn-SC surface has been predicted by molecular dynamics computation.[24] As indicated in Figure 4 with an arrow and a broken line, one pair of crystalline axes of the Pn-SC and C_{60} overlayer coincides to this direction. The reason for the anisotropic diffusion can be attributed to the atomic arrangement on the top surface of the Pn-SC. Submolecular scale corrugation at the solid surface of organic molecules is known to induce the alignment of a second molecular material,[8,15] and such a templated growth of polymer chains has actually been observed on the surfaces of polyacene single crystals.[49,50] These observations imply that the crystallization of the adsorbed C_{60} molecules is initiated on the "furrows" running along the [1$\bar{1}$0] direction of the Pn-SC surface. It should explicitly be noted that Figure 4 only represents the inter-relation between two lattices of the Pn-SC and C_{60} and does not illustrate the lateral displacement of individual C_{60} molecules with respect to the pentacene molecules. Nevertheless, an in-depth understanding of the intermolecular displacement at this heterojunction is still an open question to be investigated in further studies of theoretical modeling of the surface force field[8,13,18,21,51] as well as using experimental techniques of higher accuracy, for example, crystal truncation rod measurements[36] or molecular resolution scanning probe microscopy.

4. CONCLUSION

Heteroepitaxial growth of a C_{60} crystalline overlayer on a pentacene single crystal surface was experimentally demonstrated. The surface morphologies observed by nc-AFM imply the trapping of the adsorbed C_{60} molecules at step edges of the Pn-SC and the formation of C_{60} islands with a well-ordered internal structure within the terraces at an early stage in the formation of the interface. The XRR results substantiate the crystallinity of the C_{60} overlayer and indicate the formation of the (111)-oriented fcc C_{60} crystal with a crystal structure similar to the bulk C_{60} phase. 2D-GIXD measurements clearly demonstrate that the C_{60} crystalline overlayer is not polycrystalline but that its crystal axes point to specific directions suggesting in-plane heteroepitaxy. The crystallographic interrelation in this molecular p−n heterojunction is accurately analyzed based on 2D-GIXD results to reveal a close matching of one point of the hexagonal C_{60} lattice with a lattice point of the Pn-SC [1$\bar{1}$0].

■ ASSOCIATED CONTENT

Supporting Information

The Supporting Information is available free of charge on the ACS Publications website at DOI: 10.1021/acsami.6b02744.

Experimental setup of the 2D-GIXD measurements, construction of the fcc C_{60} stacks and their variants, absence of morphological transformation by air exposure, Indexing of the Pn-SC surface, coincidence of the reciprocal points (PDF)

■ AUTHOR INFORMATION

Corresponding Author

*E-mail: nkym@rs.tus.ac.jp.

Notes

The authors declare no competing financial interest.

■ ACKNOWLEDGMENTS

A part of this work was done under the approval of JASRI (Proposal 2014B1641, 2015A1685, and 2015B1624) (as collaborating proposals with Keysight Technologies) and of the Paul Scherrer Institute (Proposals 20141165 and 20150468). Financial supports from KAKENHI [15H05498, 25288114, and 25870034] of the Japan Society for the Promotion of Science (JSPS), JGC-S Scholarship Foundation, Izumi Science and Technology Foundation, G-COE/TA-KUETSU Programs of Chiba University [G-3, MEXT], and the Start-up Fund for Young Faculties of Tokyo University of Science are gratefully acknowledged. This work was also partially supported by Casio Science Promotion Foundation, the Helmholtz Energy Alliance "Hybrid Photovoltaics", and the Deutsche Forschungsgemeinschaft (DFG).

DOI: 10.1021/acsami.6b02744
ACS Appl. Mater. Interfaces 2016, 8, 13499−13505

REFERENCES

(1) Tang, C. W. Two-layer Organic Photovoltaic Cell. *Appl. Phys. Lett.* **1986**, *48*, 183−185.
(2) Hiramoto, M.; Fujiwara, H.; Yokoyama, M. Three-layered Organic Solar Cell with a Photoactive Interlayer of Codeposited Pigments. *Appl. Phys. Lett.* **1991**, *58*, 1062−1064.
(3) Hiramoto, M.; Fujiwara, H.; Yokoyama, M. P-I-N like Behavior in Three-Layered Organic Solar Cells Having a Co-Deposited Interlayer of Pigments. *J. Appl. Phys.* **1992**, *72*, 3781−3787.
(4) Yu, G.; Gao, J.; Hummelen, J. C.; Wudl, F.; Heeger, A. J. Polymer Photovoltaic Cells - Enhanced Efficiencies Via a Network of Internal Donor-Acceptor Heterojunctions. *Science* **1995**, *270*, 1789−1791.
(5) Peumans, P.; Uchida, S.; Forrest, S. R. Efficient Bulk Heterojunction Photovoltaic Cells Using Small-Molecular-Weight Organic Thin Films. *Nature* **2003**, *425*, 158−162.
(6) Tumbleston, J. R.; Collins, B. A.; Yang, L.; Stuart, A. C.; Gann, E.; Ma, W.; You, W.; Ade, H. The Influence of Molecular Orientation on Organic Bulk Heterojunction Solar Cells. *Nat. Photonics* **2014**, *8*, 385−391.
(7) Hinderhofer, A.; Schreiber, F. Organic-Organic Heterostructures: Concepts and Applications. *ChemPhysChem* **2012**, *13*, 628−643.
(8) Campione, M.; Sassella, A.; Moret, M.; Papagni, A.; Trabattoni, S.; Resel, R.; Lengyel, O.; Marcon, V.; Raos, G. Organic-Organic Epitaxy of Incommensurate Systems: Quaterthiophene on Potassium Hydrogen Phthalate Single Crystals. *J. Am. Chem. Soc.* **2006**, *128*, 13378−13387.
(9) Sassella, A.; Campione, M.; Raimondo, L.; Tavazzi, S.; Borghesi, A.; Goletti, C.; Bussetti, G.; Chiaradia, P. Epitaxial Growth of Organic Heterostructures: Morphology, Structure, and Growth Mode. *Surf. Sci.* **2007**, *601*, 2571−2575.
(10) Sassella, A.; Campione, M.; Borghesi, A. Organic Epitaxy. *Riv. Nuovo Cimento* **2008**, *31*, 457−490.
(11) Yang, J.; Yan, D. Weak Epitaxy Growth of Organic Semiconductor Thin Films. *Chem. Soc. Rev.* **2009**, *38*, 2634−2645.
(12) Simbrunner, C.; Quochi, F.; Hernandez-Sosa, G.; Oehzelt, M.; Resel, R.; Hesser, G.; Arndt, M.; Saba, M.; Mura, A.; Bongiovanni, G.; Sitter, H. Organic-Organic Heteroepitaxy of Red-, Green-, and Blue-Emitting Nanofibers. *ACS Nano* **2010**, *4*, 6244−6250.
(13) Raimondo, L.; Moret, M.; Campione, M.; Borghesi, A.; Sassella, A. Unique Orientation of Organic Epitaxial Thin Films: The Role of Intermolecular Interactions at the Interface and Surface Symmetry. *J. Phys. Chem. C* **2011**, *115*, 5880−5885.
(14) Huang, L.; Zhu, F.; Liu, C.; Treske, U.; Grobosch, M.; Tian, H.; Zhang, J.; Geng, Y.; Knupfer, M.; Yan, D. Crystalline Organic Heterostructures Engineering Based on Vanadyl Phthalocyanine and Rod-Like Conjugated Organic Semiconductors with Selected Central Groups. *Adv. Funct. Mater.* **2012**, *22*, 4598−4607.
(15) Sassella, A. Organic Epitaxial Layers on Organic Substrates. *Cryst. Res. Technol.* **2013**, *48*, 840−848.
(16) Noever, S. J.; Fischer, S.; Nickel, B. Dual Channel Operation upon N-Channel Percolation in a Pentacene-C_{60} Ambipolar Organic Thin Film Transistor. *Adv. Mater.* **2013**, *25*, 2147−2151.
(17) Nakayama, Y.; Niederhausen, J.; Machida, S.; Uragami, Y.; Kinjo, H.; Vollmer, A.; Rabe, J. P.; Koch, N.; Ishii, H. Valence Band Structure of Rubrene Single Crystals in Contact with an Organic Gate Dielectric. *Org. Electron.* **2013**, *14*, 1825−1832.
(18) Trabattoni, S.; Moret, M.; Campione, M.; Raimondo, L.; Sassella, A. Epitaxial Growth of Organic Semiconductor Polymorphs on Natural Amino Acid Single Crystals. *Cryst. Growth Des.* **2013**, *13*, 4268−4278.
(19) Miyadera, T.; Mitsuta, H.; Ohashi, N.; Taima, T.; Zhou, Y.; Yamanari, T.; Yoshida, Y. Heteroepitaxial Growth of C_{60} on Tetracene Single Crystal. *MRS Online Proc. Libr.* **2013**, *1501*, 1436561.
(20) Simbrunner, C.; Schwabegger, G.; Resel, R.; Dingemans, T.; Quochi, F.; Saba, M.; Mura, A.; Bongiovanni, G.; Sitter, H. Heteroepitaxy of Organic Nanofibers: Example of Ternaphthalene on p-Hexaphenyl. *Cryst. Growth Des.* **2014**, *14*, 5719−5728.
(21) Trabattoni, S.; Raimondo, L.; Campione, M.; Braga, D.; Holmberg, V. C.; Norris, D. J.; Moret, M.; Ciavatti, A.; Fraboni, B.; Sassella, A. Substrate Selection for Full Exploitation of Organic Semiconductor Films: Epitaxial Rubrene on β-Alanine Single Crystals. *Adv. Mater. Interfaces* **2015**, *2*, 1500423.
(22) Yoo, S.; Domercq, B.; Kippelen, B. Efficient Thin-Film Organic Solar Cells Based on pentacene/C_{60} Heterojunctions. *Appl. Phys. Lett.* **2004**, *85*, 5427.
(23) Itaka, K.; Yamashiro, M.; Yamaguchi, J.; Haemori, M.; Yaginuma, S.; Matsumoto, Y.; Kondo, M.; Koinuma, H. High-Mobility C_{60} Field-Effect Transistors Fabricated on Molecular- Wetting Controlled Substrates. *Adv. Mater.* **2006**, *18*, 1713−1716.
(24) Cantrell, R.; Clancy, P. A Computational Study of Surface Diffusion of C_{60} on Pentacene. *Surf. Sci.* **2008**, *602*, 3499−3505.
(25) Salzmann, I.; Duhm, S.; Opitz, R.; Johnson, R. L.; Rabe, J. P.; Koch, N. Structural and Electronic Properties of Pentacene-Fullerene Heterojunctions. *J. Appl. Phys.* **2008**, *104*, 114518.
(26) Verlaak, S.; Beljonne, D.; Cheyns, D.; Rolin, C.; Linares, M.; Castet, F.; Cornil, J.; Heremans, P. Electronic Structure and Geminate Pair Energetics at Organic-Organic Interfaces: The Case of Pentacene/C_{60} Heterojunctions. *Adv. Funct. Mater.* **2009**, *19*, 3809−3814.
(27) Conrad, B. R.; Tosado, J.; Dutton, G.; Dougherty, D. B.; Jin, W.; Bonnen, T.; Schuldenfrei, A.; Cullen, W. G.; Williams, E. D.; Reutt-Robey, J. E.; Robey, S. W. C_{60} Cluster Formation at Interfaces with Pentacene Thin-Film Phases. *Appl. Phys. Lett.* **2009**, *95*, 213302.
(28) Linares, M.; Beljonne, D.; Cornil, J.; Lancaster, K.; Brédas, J.-L.; Verlaak, S.; Mityashin, A.; Heremans, P.; Fuchs, A.; Lennartz, C.; Idé, J.; Méreau, R.; Aurel, P.; Ducasse, L.; Castet, F. On the Interface Dipole at the Pentacene−Fullerene Heterojunction: A Theoretical Study. *J. Phys. Chem. C* **2010**, *114*, 3215−3224.
(29) Breuer, T.; Witte, G. Diffusion-Controlled Growth of Molecular Heterostructures: Fabrication of Two-, One-, and Zero-Dimensional C_{60} Nanostructures on Pentacene Substrates. *ACS Appl. Mater. Interfaces* **2013**, *5*, 9740−9745.
(30) Fu, Y.-T.; Risko, C.; Brédas, J.-L. Intermixing at the Pentacene-Fullerene Bilayer Interface: A Molecular Dynamics Study. *Adv. Mater.* **2013**, *25*, 878−882.
(31) Breuer, T.; Karthäuser, A.; Witte, G. Effects of Molecular Orientation in Acceptor-Donor Interfaces between Pentacene and C_{60} and Diels-Alder Adduct Formation at the Molecular Interface. *Adv. Mater. Interfaces* **2016**, DOI: 10.1002/admi.201500452.
(32) Rao, A.; Wilson, M. W. B.; Hodgkiss, J. M.; Albert-Seifried, S.; Bässler, H.; Friend, R. H. Exciton Fission and Charge Generation via Triplet Excitons in pentacene/C_{60} Bilayers. *J. Am. Chem. Soc.* **2010**, *132*, 12698−12703.
(33) Wilson, M. W. B.; Rao, A.; Ehrler, B.; Friend, R. H. Singlet Exciton Fission in Polycrystalline Pentacene: From Photophysics toward Devices. *Acc. Chem. Res.* **2013**, *46*, 1330−1338.
(34) Yamamoto, M.; Nakayama, Y.; Uragami, Y.; Kinjo, H.; Mizuno, Y.; Mase, K.; Koswattage, K. R.; Ishii, H. Electronic Structures of a Well-Dened Organic Hetero-Interface: C_{60} on Pentacene Single Crystal. *e-J. Surf. Sci. Nanotechnol.* **2015**, *13*, 59−64.
(35) Mattheus, C. C.; Dros, A. B.; Baas, J.; Oostergetel, G. T.; Meetsma, A.; De Boer, J. L.; Palstra, T. T. M. Identification of Polymorphs of Pentacene. *Synth. Met.* **2003**, *138*, 475−481.
(36) Schiefer, S.; Huth, M.; Dobrinevski, A.; Nickel, B. Determination of the Crystal Structure of Substrate-Induced Pentacene Polymorphs in Fiber Structured Thin Films. *J. Am. Chem. Soc.* **2007**, *129*, 10316−10317.
(37) Northrup, J. E.; Tiago, M. L.; Louie, S. G. Surface Energetics and Growth of Pentacene. *Phys. Rev. B: Condens. Matter Mater. Phys.* **2002**, *66*, 121404.
(38) Nakayama, Y.; Uragami, Y.; Yamamoto, M.; Yonezawa, K.; Mase, K.; Kera, S.; Ishii, H.; Ueno, N. High-Resolution Core-Level Photoemission Measurements on the Pentacene Single Crystal Surface Assisted by Photoconduction. *J. Phys.: Condens. Matter* **2016**, *28*, 094001.
(39) Willmott, P. R.; Meister, D.; Leake, S. J.; Lange, M.; Bergamaschi, A.; Böge, M.; Calvi, M.; Cancellieri, C.; Casati, N.; Cervellino, A.; Chen, Q.; David, C.; Flechsig, U.; Gozzo, F.; Henrich, B.; Jäggi-Spielmann, S.; Jakob, B.; Kalichava, I.; Karvinen, P.;

DOI: 10.1021/acsami.6b02744
ACS Appl. Mater. Interfaces 2016, 8, 13499−13505

Krempasky, J.; Lüdeke, A.; Lüscher, R.; Maag, S.; Quitmann, C.; Reinle-Schmitt, M. L.; Schmidt, T.; Schmitt, B.; Streun, A.; Vartiainen, I.; Vitins, M.; Wang, X.; Wullschleger, R. The Materials Science Beamline Upgrade at the Swiss Light Source. *J. Synchrotron Radiat.* **2013**, *20*, 667−682.
(40) Ritley, K. A.; Krause, B.; Schreiber, F.; Dosch, H. A Portable Ultrahigh Vacuum Organic Molecular Beam Deposition System for in Situ X-Ray Diffraction Measurements. *Rev. Sci. Instrum.* **2001**, *72*, 1453−1457.
(41) Hosokai, T.; Gerlach, A.; Hinderhofer, A.; Frank, C.; Ligorio, G.; Heinemeyer, U.; Vorobiev, A.; Schreiber, F. Simultaneous in Situ Measurements of X-Ray Reflectivity and Optical Spectroscopy during Organic Semiconductor Thin Film Growth. *Appl. Phys. Lett.* **2010**, *97*, 063301.
(42) Cantrell, R. A.; James, C.; Clancy, P. Computationally Derived Rules for Persistence of C_{60} Nanowires on Recumbent Pentacene Bilayers. *Langmuir* **2011**, *27*, 9944−9954.
(43) Dorset, D. L.; McCourt, M. P. Disorder and the Molecular Packing of C_{60} Buckminsterfullerene: A Direct Electron-Crystallographic Analysis. *Acta Crystallogr., Sect. A: Found. Crystallogr.* **1994**, *50*, 344−351.
(44) Mattheus, C. C.; Dros, A. B.; Baas, J.; Meetsma, A.; de Boer, J. L.; Palstra, T. T. Polymorphism in Pentacene. *Acta Crystallogr., Sect. C: Cryst. Struct. Commun.* **2001**, *57*, 939−941.
(45) Hooks, D. E.; Fritz, T.; Ward, M. D. Epitaxy and Molecular Organization on Solid Substrates. *Adv. Mater.* **2001**, *13*, 227−241.
(46) Koma, A. New Epitaxial Growth Method for Modulated Structures Using Van Der Waals Interactions. *Surf. Sci.* **1992**, *267*, 29−33.
(47) Forrest, S. R. Ultrathin Organic Films Grown by Organic Molecular Beam Deposition and Related Techniques. *Chem. Rev.* **1997**, *97*, 1793−1896.
(48) Novaco, A. D.; McTague, J. P. Orientational Epitaxy - the Orientational Ordering of Incommensurate Structures. *Phys. Rev. Lett.* **1977**, *38*, 1286−1289.
(49) Wittmann, J. C.; Lotz, B. Epitaxial Crystallization of Polyethylene on Organic Substrates: A Reappraisal of the Mode of Action of Selected Nucleating Agents. *J. Polym. Sci., Polym. Phys. Ed.* **1981**, *19*, 1837−1851.
(50) Wittmann, J. C.; Lotz, B. Epitaxial Crystallization of Polymers on Organic and Polymeric Substrates. *Prog. Polym. Sci.* **1990**, *15*, 909−948.
(51) Zhang, Y.; Forrest, S. R. Mechanisms of Quasiepitaxial Ordering at Organic Molecular Thin Film Interfaces. *Phys. Rev. Lett.* **1993**, *71*, 2765−2768.

DOI: 10.1021/acsami.6b02744
ACS Appl. Mater. Interfaces 2016, 8, 13499−13505